Microelectronic Engineering 174 (2017) 20–23

Contents lists available at ScienceDirect

Microelectronic Engineering

journal homepage: www.elsevier.com/locate/mee

Research paper

Fabrication and development of high brightness nano-aperture ion source

Xinxin Xu [a], Rudy Pang [a,b], P. Santhana Raman [a,b], Rajasekaran Mariappan [a], Anjam Khursheed [b], Jeroen A. van Kan [a,*]

[a] Centre for Ion Beam Applications, Department of Physics, National University of Singapore, 117542, Singapore
[b] Department of Electrical and Computer Engineering, National University of Singapore, 117583, Singapore

ARTICLE INFO

Article history:
Received 14 October 2016
Received in revised form 25 November 2016
Accepted 14 December 2016
Available online 18 December 2016

Keywords:
Proton beam writing
Nano-aperture ion source
Brightness

ABSTRACT

Nano-aperture ion source (NAIS) is a potential candidate to be a part of a sub-10 nm proton beam writing (PBW) system. To improve the performance of our prototype NAIS, currently we have modified the fabrication process. Through integrating the ionization chamber into the silicon nitride membranes and reducing the size of double-aperture, we have improved the overall performance of NAIS. The reduced brightness from this modified NAIS was obtained to be 9.1×10^3 A/(m^{2}srV) for an Ar$^+$ beam. Limitations and further improvements of the current design are discussed in the paper.

© 2016 Elsevier B.V. All rights reserved.

1. Introduction

Proton beam writing (PBW) is a direct-write lithographic technique developed in the Centre for Ion Beam Applications, National University of Singapore (CIBA-NUS), which employs focused protons, for fabricating three-dimensional nano-structures [1–3]. Compared with electron beam lithography (EBL), the advantage of PBW is that a proton is ~1800 times heavier than an electron, which makes a proton to transfer less energy to secondary electrons and can penetrate straighter into the material, depositing a constant energy along its path in the resist [4]. With these unique features, PBW can fabricate nano-structures without proximity effects and having smooth sidewalls [3,5]. Currently, the performance of PBW in terms of spot size and throughput is limited by low brightness ~20 A/(m^{2}srV) of the radio frequency (RF) ion source, available in PBW systems [6,7]. Therefore a high brightness ion source is the key to further improve the performance of PBW system.

The reduced brightness is an important parameter to exemplify beam quality, like beam current density, beam angular spread, and beam energy spread [8,9]. Reducing the virtual source size is a practical way to obtain high brightness ion source [10]. High brightness ion sources, like liquid metal ion source (LMIS) and gas field ionization source (GFIS), have small virtual source sizes. LMIS is the most widely used high brightness ion source, which has a liquid metal reservoir on top of a sharp tip [11–13]. A strong electric field is used to pull the liquid metal to a sharp electrospray cone, known as Taylor cone [14]. Meanwhile this strong electric field also generates ions at the tip of the Taylor cone by field evaporation. The most common LMIS is Ga-LMIS but several other metals (e.g. Al, In, Sn, Cs, Bi, Au) as well as alloy metals (Au-Si, Au-Ge, Si-Be-Au, Ni-B-Pt) are also used [11]. The typical virtual source size of Ga-LMIS is about 50 nm and the reduced brightness is about 10^6 A/(m^{2}srV) with typical energy spread of around 5 eV [11,15,16]. However, the choice of ions from the LMIS is limited to metallic ions, and the energy spread results in high chromatic aberration. GFIS has recently emerged as a credible choice for high brightness ion source, which is based on the field ionization created by strong electric field [17–19]. A strong electric field is concentrated at the apex of a pyramidal tip, which terminates with three atoms. GFIS has been mostly used for generating He and Ne ions [19,20]. For He-GFIS, the reduced brightness can reach as high as 10^9 A/(m^{2}srV) with a 1 eV energy spread [21]. The small virtual source size (<1 nm), due to the three-atom terminated tip, results in having high brightness [22,23]. While the GFIS can deliver an extremely high brightness ion beam, it is limited by the variety of available ion species. Another approach to obtain high brightness ion source is to reduce the beam angular spread, which can be achieved by reducing the source operating temperature (<100 μK). Such ion sources, operating at low temperatures (usually achieved by laser cooling), are called cold atom ion source. These ion sources have a theoretical reduced brightness of around 10^7 A/(m^{2}srV), with <0.5 eV energy spread [24–27]. Using laser-cooled Cr atoms and Li atoms, beams with reduced brightness of 2.25×10^4 A/(m^{2}srV) [28] and 6×10^3 A/(m^{2}srV) [29] have been achieved respectfully. Although these ion sources can deliver high brightness ion beams, they are not designed to produce high brightness proton beams. A nano-aperture

* Corresponding author.
E-mail address: phyjavk@nus.edu.sg (J.A. van Kan).

http://dx.doi.org/10.1016/j.mee.2016.12.009
0167-9317/© 2016 Elsevier B.V. All rights reserved.

ion source (NAIS) with an estimated brightness of 10^6 A/(m^2srV) has been reported by the Charged Particle Optics group at Delft University of Technology [30]. This NAIS is expected to generate high brightness proton beams. Thus NAIS is a prospective candidate for a sub-10 nm PBW system, which can deliver high throughput. This system is expected to achieve writing speed comparable to those in EBL without the unwanted proximity effect [31].

2. NAIS concept and fabrication process

The mechanism of NAIS is to extract ions from electron-gas collision, which creates ionization, in a sub-micron ionization chamber, as shown in Fig. 1. This is a simple and reliable ionization approach to generate various types of ions. The superiority of NAIS is to reduce the virtual source size to sub-micrometer while maintaining a strong electric field (~10^7 V/m) with a small chip bias (~1 V), resulting in an ion energy spread of <1 eV [30]. Furthermore, the versatility of NAIS makes it convenient to select different ion species spanning from low Z to heavy Z gaseous elements, catering to different applications. All these virtues require a critical ionization chamber to deliver high brightness ions. We have shown a brightness of about 750 A/m^2srV for Ar^+ with the NAIS in our preliminary experiments [32]. These experiments were performed in a scanning electron microscope (SEM), which serves as a source to supply the electron beam for gas ionization. The ion brightness of this prototype NAIS was mainly limited by the poor brightness of the injected electron beam, large dimension (600 nm height) of the ionization chamber, thick silicon nitride membranes (1 μm), and a large double-aperture (1.5 μm) [32,33]. Therefore, a modified ionization chamber is fabricated to further improve the performance of NAIS.

A 7 mm × 1 mm × 300 nm NAIS ionization chamber has been fabricated by gluing two silicon nitride membranes, as shown in Fig. 1, using a microelectromechanical system (MEMS) technique. The step-by-step fabrication procedure is shown in Fig. 2. The ionization chamber was formed from the top and bottom chips of a 400 μm thick <100> silicon wafer. The silicon wafer was double-side-polished with a 280 nm low-pressure chemical vapor deposited (LPCVD) silicon nitride on both sides. To enable batch production, the top and bottom chips were designed to be identical to each other. In order to create the gas inlet, electron beam inlet, and ion beam outlet (referred as double-aperture) windows, the front side of the wafer was spin-coated with 2.5 μm thick AZ 1518 photoresist followed with 50 s soft bake at 100 °C. Subsequently, the photoresist was exposed with a 405 nm laser to pattern the windows. The exposed windows were developed in AZ 400k developer diluted to 1:4 with DI water for 1 min. The patterned windows were then transferred to silicon nitride through deep reactive ion etching (DRIE) with process parameters of 48 sccm CHF_3, 5 sccm O_2, 15 Pa pressure, and 250 W RF power, as shown in Fig. 2(a). This is followed by stripping of the residual AZ 1518 resist in acetone, opening up access holes by etching the exposed Si in KOH (Fig. 2(b)) and creating a free-standing silicon nitride membrane, and electrode formation by depositing a conductive layer (10 nm Cr and 20 nm Au) via magnetron

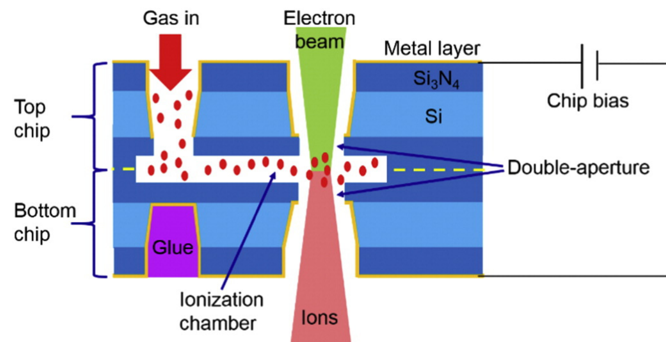

Fig. 1. Schematic of modified NAIS.

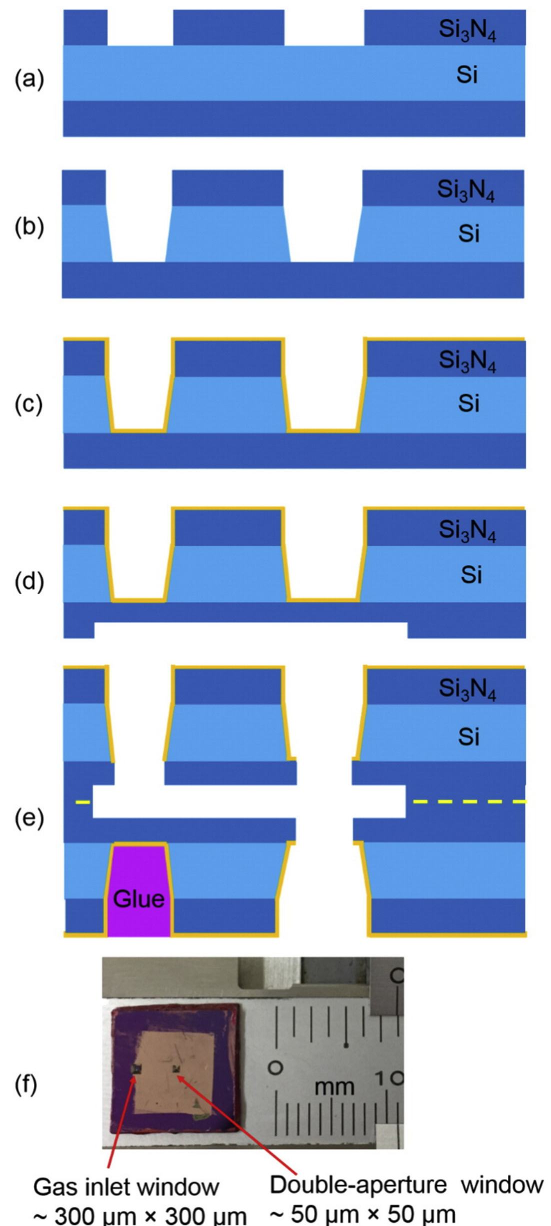

Fig. 2. Depiction of the NAIS chip fabrication process: (a) DRIE to create gas inlet and double-aperture windows on silicon nitride. (b) KOH etching to reach the bottom side of silicon nitride membrane. (c) 10 nm Cr + 20 nm Au deposited by magnetron sputtering for electrode. (d) 150 nm depth ionization spacer created by DRIE. (e) NAIS chip bonded with two individual chips and FIB-milled for creating gas inlet aperture and double-aperture. The diameter of the double-aperture is 500 nm. (f) A fabricated NAIS chip with a 300 μm × 300 μm gas inlet and 50 μm × 50 μm double-aperture windows.

sputtering on the processed side of the wafers (Fig. 2(c)). On completing the process steps at the front side of the wafer, the fabrication process was carried out at the back side of the wafer to create the ionization chamber. For the back side, the wafer was spin-coated with 5 μm thick AR-P 3250 photoresist followed by 2 min soft bake at 95 °C. The ionization channel pattern was exposed using a 365 nm ultraviolet (UV) and developed in AR 300-26 developer diluted to 3:2 in DI water for 1.5 min. The back side of silicon nitride membrane was dry-etched down to 150 nm depth in a selected window (see Fig. 2(d)). The two chips were then bonded face to face (see Fig. 2(e)) to create an ionization chamber with a dimension of 7 mm × 1 mm × 300 nm. The gas inlet aperture and the double-aperture were created with the aid of gallium FIB milling (FEI Quanta Dual Beam). The double-aperture size was set to be 500 nm. Finally, the larger opening at the bottom side of the

NAIS chip was sealed off using vacuum glue for better gas pressure within.

3. Result and discussion

From an experimental standpoint, the reduced brightness is defined as [34,35]

$$B_r = \frac{I_a}{A_s \Omega V} = \frac{I_a}{A_s \frac{A_a}{L^2} V} \tag{1}$$

where I_a is the ion beam current, A_s is the virtual source area, Ω is the solid angle which defines the beam divergence, V is the beam acceleration potential, A_a is the angular aperture area, and L is the distance between virtual source and the angular aperture.

To set up the reduced brightness measurement, a JEOL JSM-5600 tungsten scanning electron microscopy (SEM) was used as an electron injector. This SEM was operated at 1 keV with an electron beam current of a few tens of nA. The brightness measurement setup was positioned inside the SEM chamber as shown in Fig. 3. Focused electrons were injected into the ionization chamber through double-aperture to ionize the gas. A regulator valve was used to control inlet gas pressure between 1 mbar and 1 bar. The reduced brightness measurement was performed with argon ions (Ar^+ 95%, the rest are Ar^{n+}, n = 2 to 4) [36] to examine the performance of this NAIS. The electric field inside the NAIS chamber was varied by tuning the bias across the NAIS chip from 0 to 100 V. The extractor was set at a negative potential (<-1 kV) to accelerate the ion beam and also to prevent the injected electron beam to travel further downstream into the setup. An angular aperture (95 μm × 112 μm, 10 mm downstream from the NAIS chip) to define the solid angle was kept at the same potential as the extractor. The angular aperture was fabricated by a similar process as adopted for the NAIS chip's double aperture. This angular aperture was mounted on a piezo-XY linear stage (SmarAct® SLC-1720-S-HV) and scanned through the beam to find the peak axial beam current as measured in a Faraday cup. Downstream of the angular aperture, a suppressor electrode (at equipotential with the extractor) was used to maintain a field-free region for ions. At the end of this setup, the Faraday cup was biased at −90 V to aid ion beam-landing.

It was reported that increasing the inlet gas pressure in NAIS results in generating a higher ion beam current [33]. Accordingly, in the current experiment the inlet Ar gas pressure was set to be 860 mbar. The Knudsen number K_n, which is defined as the ratio of the molecular mean free path length to the ionization chamber height, under current conditions

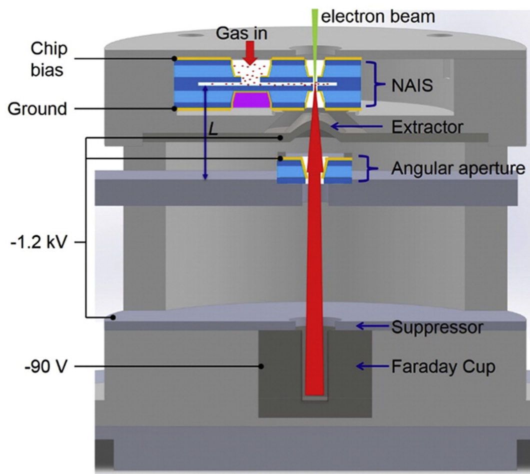

Fig. 3. Schematic setup of NAIS brightness measurement, carried out inside a JEOL JSM-5600 tungsten SEM.

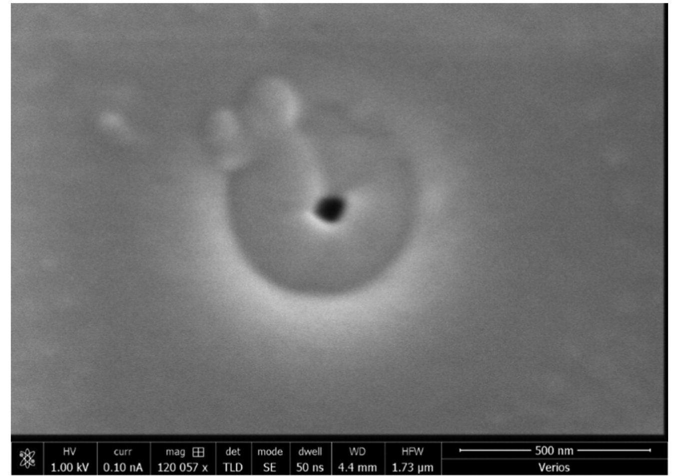

Fig. 4. SEM image (taken by field emission SEM, FEI Verios 460) of the double-aperture after being used.

is around 0.2. Further increase in the inlet gas pressure might lead to undesired ion-gas collisions. Chip bias is used to repel ions out of NAIS chamber. This chip bias was varied from 0 to 100 V to obtain maximum output current from the NAIS. In the current NAIS's mechanical design, a misalignment of about 100 μm is inherited between the double-aperture and the extractor, resulting in off-axis aberration. This can cause a negative influence on the reduced brightness measurement, especially for high extraction potential [37]. Therefore the extractor potential was deemed to be optimal at −1.2 kV. With the following parameters: inlet gas pressure of 860 mbar, chip bias of 23 V, and an extractor potential of −1.2 kV, an axial peak current of 230 pA has been observed. On substituting these values in Eq. (1), a reduced brightness for Ar^+ is found to be 9.1×10^3 A/(m^{2}srV). Here, the value of virtual source size was considered to be the same as the double-aperture size (500 nm). Since the virtual source size of a planar emitter is expected to be smaller than the real source size [32], the current reported reduced brightness can be much higher.

The injected electron beam, used to ionize Ar gas molecules, has a relatively larger spot size with respect to the double-aperture. This induces severe clogging on the surface of the NAIS chip at the entrance of double-aperture (as shown in Fig. 4), due to electron beam-induced deposition (EBID). To prevent this clogging effect, a fine focused electron beam is required.

4. Conclusion

The NAIS ionization chamber is very critical to achieve a high brightness ion beam. To improve the performance of the prototype NAIS [32, 33], a modified NAIS chip has been successfully fabricated and tested. This modified NAIS chip consists of an integral ionization chamber inside silicon nitride membranes. The double-aperture of this NAIS chip is now reduced to 500 nm in diameter. The fabrication process is designed for batch production using MEMS fabrication techniques. With this modified NAIS, a reduced brightness of 9.1×10^3 A/(m^{2}srV) of Ar^+ has been achieved, which is 1 order higher than the prototype NAIS [32,33] and 3 orders higher than the RF source in the existing PBW system [7]. Better mechanical alignment of NAIS chip and extractor, higher electron beam current density, determination of more appropriate virtual source size, and fine tuning of other parameters will result in enhanced reduced brightness.

Acknowledgements

We thank the advices from Dr. C. W. Hagen and Dr. P. Kruit from CPO-TUD. We also thank Dr. S.K. Vajandar from our group for helpful

discussion. This research was funded by the National Research Foundation (NRF) Competitive Research Programme (CRP) reference # NRF-CRP13-2014-04.

References

[1] J.A. van Kan, A.A. Bettiol, F. Watt, Proton beam writing of three-dimensional nanostructures in hydrogen silsesquioxane, Nano Lett. 6 (3) (2006) 579–582.
[2] F. Watt, M.B. Breese, A.A. Bettiol, J.A. van Kan, Proton beam writing, Mater. Today 10 (6) (2007) 20–29.
[3] J.A. Van Kan, A.A. Bettiol, F. Watt, Three-dimensional nanolithography using proton beam writing, Appl. Phys. Lett. 83 (8) (2003) 1629–1631.
[4] C. Udalagama, A.A. Bettiol, F. Watt, Stochastic spatial energy deposition profiles for MeV protons and keV electrons, Phys. Rev. B 80 (22) (2009) 224107.
[5] J.A. Van Kan, P. Shao, K. Ansari, A.A. Bettiol, T. Osipowicz, F. Watt, Proton beam writing: a tool for high-aspect ratio mask production, Microsyst. Technol. 13 (5–6) (2007) 431–434.
[6] R. Szymanski, D.N. Jamieson, Ion source brightness and nuclear microprobe applications, Nucl. Instrum. Methods Phys. Res., Sect. B 130 (1) (1997) 80–85.
[7] J.A. Van Kan, P. Malar, A.B. De Vera, The second generation Singapore high resolution proton beam writing facility, Rev. Sci. Instrum. 83 (2) (2012) 02B902.
[8] M. Reiser, Theory and Design of Charged Particle Beams, John Wiley & Sons, 2008.
[9] J. Orloff, Handbook of Charged Particle Optics, CRC press, 2008.
[10] J. Orloff, High-resolution focused ion beams, Rev. Sci. Instrum. 64 (5) (1993) 1105–1130.
[11] J. Orloff, L. Swanson, M. Utlaut, High Resolution Focused Ion Beams: FIB and Its Applications: the Physics of Liquid Metal Ion Sources and Ion Optics and their Application to Focused Ion Beam Technology, Springer Science & Business Media, 2003.
[12] P.D. Prewett, G.L.R. Mair, Focused Ion Beams from Liquid Metal Ion Sources, Research Studies Press Ltd, 1991.
[13] R. Forbest, Understanding how the liquid-metal ion source works, Vacuum 48 (1) (1997) 85–97.
[14] G. Taylor, Disintegration of water drops in an electric field, Proc. R. Soc. Lond. A (1964) 383–397.
[15] M. Watts, Analytical model of positive resist development applied to linewidth control in optical lithography, J. Vac. Sci. Technol. B 3 (1) (1985) 434–440.
[16] C. Hagen, E. Fokkema, P. Kruit, Brightness measurements of a gallium liquid metal ion source, J. Vac. Sci. Technol. B 26 (6) (2008) 2091–2096.
[17] N.P. Economou, J.A. Notte, W.B. Thompson, The history and development of the helium ion microscope, Scanning 34 (2) (2012) 83–89.
[18] G. Hlawacek, V. Veligura, R. van Gastel, B. Poelsema, Helium ion microscopy, J. Vac. Sci. Technol. B 32 (2) (2014) 020801.
[19] B.`. Ward, J.A. Notte, N. Economou, Helium ion microscope: a new tool for nanoscale microscopy and metrology, J. Vac. Sci. Technol. B 24 (6) (2006) 2871–2874.
[20] F. Rahman, S. McVey, L. Farkas, J.A. Notte, S. Tan, R.H. Livengood, The prospects of a subnanometer focused neon ion beam, Scanning 34 (2) (2012) 129–134.
[21] R. Hill, J. Notte, B. Ward, The ALIS He ion source and its application to high resolution microscopy, Phys. Procedia 1 (1) (2008) 135–141.
[22] H.-S. Kuo, S. Hwang, T.-Y. Fu, Y.-H. Lu, C.-Y. Lin, T.T. Tsong, Gas field ion source from an Ir/W <111> single-atom tip, Appl. Phys. Lett. 92 (2008) 063106.
[23] N.G. Einspruch, S.S. Cohen, R.N. Singh, Beam Processing Technologies, Academic Press, 2014.
[24] J.J. McClelland, A.V. Steele, B. Knuffman, K.A. Twedt, A. Schwarzkopf, T.M. Wilson, Bright focused ion beam sources based on laser-cooled atoms, Appl. Phys. Rev. 3 (1) (2016) 011302.
[25] B. Knuffman, A. Steele, J. McClelland, Cold atomic beam ion source for focused ion beam applications, J. Appl. Phys. 114 (4) (2013) 044303.
[26] S. Van der Geer, M. Reijnders, M. de Loos, E. Vredenbregt, P. Mutsaers, O. Luiten, Simulated performance of an ultracold ion source, J. Appl. Phys. 102 (9) (2007) 094312.
[27] J.L. Hanssen, J.J. McClelland, E. Dakin, M. Jacka, Laser-cooled atoms as a focused ion-beam source, Phys. Rev. A 74 (6) (2006) 063416.
[28] J.L. Hanssen, S.B. Hill, J. Orloff, J.J. McClelland, Magneto-optical-trap-based, high brightness ion source for use as a nanoscale probe, Nano Lett. 8 (9) (2008) 2844–2850.
[29] K.A. Twedt, L. Chen, J.J. McClelland, Scanning ion microscopy with low energy lithium ions, Ultramicroscopy 142 (2014) 24–31.
[30] D.S. Jun, V.G. Kutchoukov, P. Kruit, Ion beams in SEM: an experiment towards a high brightness low energy spread electron impact gas ion source, J. Vac. Sci. Technol. B 29 (6) (2011) 06F603.
[31] X. Xu, N. Liu, P.S. Raman, S. Qureshi, R. Pang, A. Khursheed, J.A. van Kan, Design considerations for a compact proton beam writing system aiming for fast sub-10 nm direct write lithography, Nucl. Instrum. Methods Phys. Res., Sect. B (2016) http://dx.doi.org/10.1016/j.nimb.2016.12.031 (in press).
[32] N. Liu, X. Xu, R. Pang, P.S. Raman, A. Khursheed, J.A. van Kan, Brightness measurement of an electron impact gas ion source for proton beam writing applications, Rev. Sci. Instrum. 87 (2) (2016) 02A903.
[33] N. Liu, P.S. Raman, X. Xu, H.M. Tan, A. Khursheed, J.A. van Kan, Development of ion sources: towards high brightness for proton beam writing applications, Nucl. Instrum. Methods Phys. Res., Sect. B 348 (2015) 23–28.
[34] L. Reimer, Scanning Electron Microscopy: Physics of Image Formation and Microanalysis, IOP Publishing, 2000.
[35] M. Breese, D. Jamieson, P. King, Materials Analysis with a Nuclear Microprobe, Wiley, New York, 1996.
[36] R. Rejoub, B. Lindsay, R. Stebbings, Determination of the absolute partial and total cross sections for electron-impact ionization of the rare gases, Phys. Rev. A 65 (4) (2002) 042713.
[37] D.W. Heddle, Electrostatic Lens Systems, CRC Press, 2000.